RESEARCH ARTICLE OPEN ACCESS

MODE II FRACTURE PARAMETERS FOR VARIOUS SIZES OF BEAMS IN PLAIN CONCRETE

Darsigunta Seshaiah
Structural Engineering Studying M.Tech In Chinthalapudi Engineering College Roll No: 137r1d8703

ABSTRACT
Blended aggregate in concrete and arriving at the structural properties of blended aggregate concrete is a thrust area. Pumice is very light and porous igneous rock that is formed during volcanic eruptions.Cinder is a waste material obtained from steel manufacturing units. Shear strength is a property of major significance for wide range of civil engineering materials and structures. Shear and punching shear failures particularly in deep beams, in corbels and in concrete flat slabs are considered to be more critical and catastrophic than other types of failures. This area has received greater attention in recent years. For investigating shear type of failures, from the literature it is found that double central notched (DCN) specimen geometry proposed by Prakash Desai and V.Bhaskar Desai is supposed the best suited geometry. In this present experimental investigation an attempt is made to study the Mode-II fracture property of light weight blended aggregate cement concrete combining both the pumice and cinder in different proportions, and making use of DCN test specimen geometry . By blending the pumice and cinder in different percentages of 0, 25, 50, 75 and 100 by volumeof concrete, a blended light weight aggregate concrete is prepared. By using this the property such as in plane shear strength is studied. Finally an analysis is carried out regarding Mode-II fracture properties of blended concrete. It is concluded that the Ultimate load in Mode-II is found to decrease continuously with the percentage increase in Pumice aggregate content. It is also observed that the ultimate stress in Mode II is found to increase continuously with percentage increase in cinder aggregate content.

Key Words: Cinder, light weight aggregate, Mode II fracture, shear strength, Pumice**.**

I. Introduction

Fracture mechanics is the science of studying the behavior of progressive crack extension in structures subjected to an applied load. Fracture mechanics is all about cracks, stress fields around cracks, stress intensity factors at cracks, failures due to cracks, growth rates of cracks, etc. This website covers all of these topics, beginning with some historical perspective for motivation.

The story begins way back at the turn of the 20th century with analytical solutions for stresses at holes in 1898, then at ellipses in 1913. Fracture mechanics research is considered to have officially begun in 1920 with Griffith's energy based analysis of cracks. Nevertheless, similar landmark contributions remained few and far between until World War II, when several structures that should have never failed, did. It was determined that the cause of these failures was cracks. This led to a rapid expansion of research into the areas of fracture mechanics and fatigue growth.

In 1983, the National Bureau Of Standards (now the National Institute for science and Technology) and Battelle Memorial Institute estimated the costs for failure due to fracture to be $119 billion dollars per year in1982. The dollars are important, but the cost of many failures in human life and injury is infinitely more.

Failure have occurred for many reasons, including uncertainties in the loading or environment, defects in the materials, inadequacies in design, and deficiencies in construction or maintenance. Design against fracture has a technology of its own, and this is a very active area of current research. This module will provide an introduction to an important aspect of this field, since without an understanding of fracture the methods in stress analysis discussed previously would be little use. The module on the dislocation basis of yield shows how the strength of structural metals particularly steel can be increased to very high levels by manipulating the microstructure so as to inhibit dislocation motion. Unfortunately, this renders the material increasingly brittle, so that cracks can form and propagate catastrophically with very little warning.

Fracture mechanics goes along with the recognition that real structures contain discontinuities which has originates in 1921 by Griffith and was for a long time applied only to metallic structures and ceramics. Concrete structures, on the other hand, have so far been successfully designed and built without any use of fracture mechanics, even though their failure process involves crack propagation.

II. HISTORICAL ASPECTS OF FRACTURE MECHANICS

For a long time, we always had some idea about the role of a crack or a notch. While cutting a tree, we would make a notch with an axe at its trunk and then pull it down with a rope. While breaking a stick we would make a small notch with a knife before bending it. Good swords were made by folding a thin metal sheet at the center line and then hammering it to make it thin again so that it could be further folded. Thus, a sword would have many layers. If a crack develops in one of the layers, it is not likely to move to another, thus making the sword very tough.

In 19th century and early part of 20th century, the entire industry was obsessed with production. Even the failure theories were developed quite late: Tresca in (1864) and Mises (1913). However, World War II accelerated the industrial production at a very rapid rate, due to unusually high demands of war. Within 6 years of the war, the know-how of aircraft making improved dramatically. Also, the ships, which were earlier made by joining plates together through the process of riveting, were changed to welded frames. Many cargo ships, known as liberty ships, were rolled out from American docks within a short span. However, soon there were complications regarding welded structures. Many of these failed in the cold temperatures of the North Atlantic Ocean. As a matter of fact some of these broke up into two parts. However, ships made by riveting plates did not display such failures. If a crack nucleated and grew in a plate, it would only slit that plate into two parts; the crack would not grow into another plate. A welded structure is a large single continuous part and therefore, if the crack becomes critical, it will run through the entire hull of the ship.

Fig 1.1: The tower bridge in London, completed in1894

III. FRACTURE MECHANICS

Fracture mechanics is the science of describing how a crack initiates and propagates under applied loads in many engineering materials like ceramics, rocks, glasses and concretes. Fracture mechanics is generally applied in the field of earth sciences such as petroleum engineering, geological engineering, mining engineering and civil engineering.

Concrete is a stone like material obtained by permitting a mixture of cement, fine aggregate and gravel or other aggregate and water to harden in forms of desires shape of the structure. Concrete has become a popular material in civil engineering for several reasons, such as the low cost of the aggregate, the accessibility of the needed materials and its high compressive strength. On the other hand concrete is a relatively brittle material with low tensile strength compared to the compressive strength.

IV. LINEAR ELASTIC FRACTURE MECHANICS (LEFM)

Linear Elastic Fracture Mechanics (LEFM) first assumes that the material is isotropic and linear elastic. Based on the assumption, the stress field near the crack tip is calculated using the theory of elasticity. When the stresses near the crack tip exceed the material fracture toughness, the crack will grow. In Linear Elastic Fracture Mechanics, most formulas are derived for either plane stresses or plane strains, associated with the three basic modes of loadings on a cracked body: opening, sliding, and tearing.

Griffith was the first to develop a method of analysis for the description of fracture in brittle materials. Griffith found that, due to small flaws and cracks, stress concentrations arise under loading, which explains why the theoretical strength is higher than the

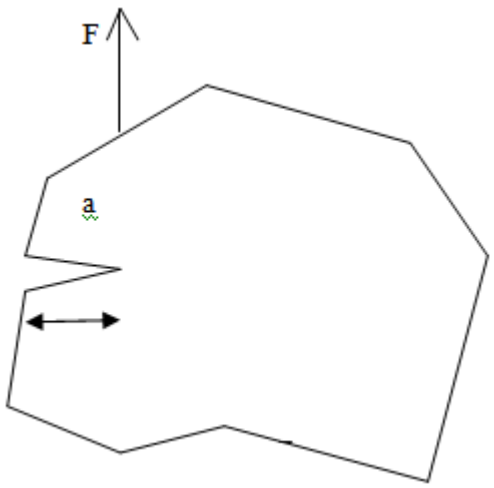

Fig 1.1: Arbitrary body with an internal crack of length a subjected to an arbitrary force F

By superposition, the potential energy of the body is given by the fracture process in concrete is given in equation

?=? $_e$ +? $_F$ +? $_k$ +? $_c$

? $_e$ = the elastic energy content in the body

? $_F$ = the potential of the external forces

? $_k$ = the total kinetic energy in the system

? $_c$ = the fracture potential

The fracture potential is the energy that dissipates during crack growth. By assuming that crack growth is only dependent on the crack length, a, the equilibrium equation can be stated, by requiring that the potential energy of the system equals to zero.

Griffith introduced a parameter, the energy release rate, G. R is the fracture resistance of the material, which is assumed to be constant in LEFM. The total potential energy of a system increases when a crack is formed because a new surface is created, thus increasing the fracture potential. However, the formation of a crack consumes an amount of energy, G, in the form of surface energy and frictional energy. If the energy release rate is larger than the energy required forming a crack.

$U_{cracked} - U_{uncracked} = - (\pi a^2 \sigma^2)/E + 4a\gamma$

Where $U_{cracked}$ and $U_{uncracked}$ are elastic energies of the plate, σ is the nominal normal stress and γ is the elastic surface energy of the plate.

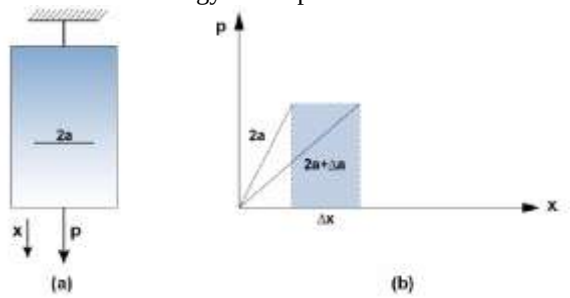

Fig.1.2 (a) Plate with crack 2a (b) Load-Displacement diagram

V. MODES OF FAILURE

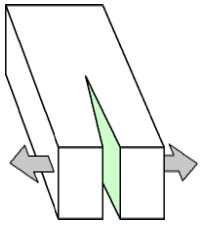

(a) Mode I (Tension, Opening)

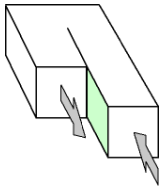

(b) **Mode II (In-Plane Shear, Sliding)**

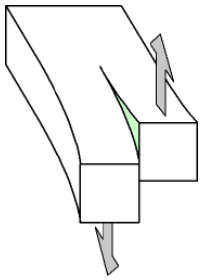

(c) **Mode III (Out-Of-Plane Shear, Tearing)**

Fig 1.3: Modes of failure

Mode I (Tension, Opening): Mode I fracture is the condition in which the crack plane is perpendicular to the direction of the applied load.

Mode II (In-Plane Shear, Sliding): Mode II fracture is the condition in which the crack plane is parallel to the direction of the applied load.

Mode III (Out-Of-Plane Shear, Tearing): Mode III fracture corresponds to a tearing mode and is only relevant in three dimensions.

An inclined crack front in a component can be modeled as a superposition of the three basic modes and then, the effect of loading by each mode can be analyzed separately. Mode I usually play a dominant role in many engineering applications and is considered to be the most dangerous. However, in certain applications, components fail through the dominant roles played by Mode II or Mode III. Any of these modes of fracture are typically assumed to initiate at the point of greatest stress concentration, which is commonly assumed to be at a flaw in the material. As shown in Figure 5, this flaw can be internal of length 2*a* or external of length *a* (Callister 2005).

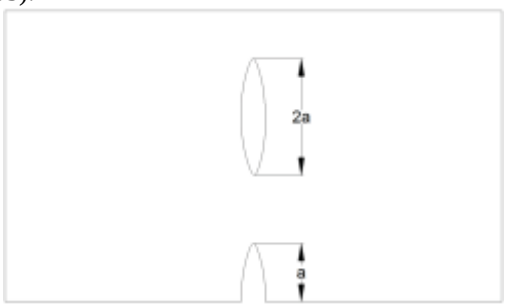

Fig. 1.4 Internal and external flaw geometry

Mode I and Mode II fracture is also referred to as an opening and in-plane shear mode, respectively. In practical calculations, only the first order term of equation is included. This is because, that for γ ? θ, the first order term approaches infinity while the higher order terms are constant or zero. Because the stress tends towards infinity when γ ? θ. A stress criterion as a failure criterion is not appropriate. For this reason, Irwin derived a relationship between the SIF and the release rate, G,

K= √G*E

The fracture criterion can thereby be written as
$K=K_c$

It should be noted that the global energy balance criteria by cite bib Griffith is equivalent to the local stress criteria by Irwin. Moreover, K_c is also referred to as the fracture toughness of the material, and is regarded as a constant in LEFM. The Griffith (1921)/ Irwin (1958) theory assumes that the stresses in vicinity of the crack tip tend to infinity. This contravenes the principle of linear elasticity, relating small strains to stresses through Hooke's law. In the fracture process zone, abbreviated FPZ, ahead of the crack tip, plastic deformation of the material occurs. Specifically for concrete de-bonding of aggregate from the cement matrix and micro cracking occurs. Moreover, cracks coalesce, branch and deflect in FPZ. To describe this highly non-linear phenomenon, non-linear fracture mechanics, abbreviated NLFM, must be adopted.

VI. STRESS INTENSITY FACTOR

Since in LEFM the state of stress near crack tip is singular, it is not possible to evaluate the stress value around crack tip accurately. In order to more accurately evaluate or predict the state of stress near crack tip Irwin and his colleagues developed a relation to calculate the amount of energy available for fracture in terms of asymptotic stress and displacement fields around a crack front in a linear elastic solid. This asymptotic relation is

$$\sigma_{ij} = \frac{k}{\sqrt{2\pi r}} (f_{ij})$$

Since σ_{ij} are the Cauchy stresses, r is t he distance from the crack tip, ? is the angle with respect to the plane of the crack geometry and loading conditions. The quantity K was called stress intensity factor. Since functions f_{ij} are dimensionless, the stress intensity factor has the units of N/mm^2. This formation is not valid for the areas very close to crack tip i.e., inside process region. This concept is a theoretical construct applicable to elastic materials and is useful for providing a failure criterion for brittle materials.

Stress intensity factor can be defined for different modes of loading (I, II, and III) and in such cases is referred to as K_I , K_{II}, and K_{III} . Stress intensity factors are related to energy release rate according to following equation for 2D problems

$G= (K^2_I/E^*) + (K^2_{II}/E^*)$

Where E* = E (young's modulus) for plane stress and $E^* = E / (1- \mu^2)$ for plane strain
μ is the Poisson's ratio

Stress and displacement equations for the centre cracked body are similar for other modes. For mode II in plane strain and far field stress $\sigma_{12}=\tau$ with $K_{II} = \tau\sqrt{}$ Πa. Stress intensity factor especially in mode II, can be used as a crack propagation criterion. There is a critical value for stress intensity factor, required to propagate the crack. This critical value determined for mode II loading in plane strain is referred to critical fracture toughness (K_{IIc}).

Mode II fractures initiation and propagation plays an important role under certain loading conditions in rock fracture mechanics. Under pure tensile, pure shear, tension- and compression-shear loading, the maximum Mode I stress intensity factor, $K_{\mathrm{I\ max}}$, is always larger than the maximum Mode II stress intensity factor, $K_{\mathrm{II\ max}}$. For brittle materials, Mode I fracture toughness, K_{IC}, is usually smaller than Mode II fracture toughness, K_{IIC}. Therefore, $K_{\mathrm{I\ max}}$ reaches K_{IC} before $K_{\mathrm{II\ max}}$ reac hes K_{IIC}, which inevitably leads to Mode I fracture. Due to inexistence of Mode II fracture under pure shear, tension- and compression-shear loading, classical mixed mode fracture criteria can only predict Mode I fracture but not Mode II fracture. A new mixed mode fracture criterion has been established for predicting Mode I or Mode II fracture of brittle materials. It is based on the examination of Mode I and Mode II stress intensity factors on the arbitrary plane θ,$K_I(\theta)$ and $K_{II}(\theta)$, varying with $\theta(-180° \square\theta\square +180°)$, no matter what kind of loading condition is applied. Mode II fracture occurs when $(K_{\mathrm{II\ max}} / K_{\mathrm{I\ max}}) > (K_{IIC} / K_{IC})$ and $K_{\mathrm{II\ max}} = K_{IIC}$ at θ_{IIC}. The validity of the new criterion is demonstrated by experimental results of shear-box testing.

VII. Size Effects In Non- Linear Elastic Fracture Mechanics

Consider a uniformly stressed panel and suppose that fracture propagates via the formation of a crack band of thickness *h*f. The load required to propagate the band follows from energy balance equation, i.e., energy available is equal to the fracture energy (the energy required for band extension). To that end, assume that due to presence of crack band the strain energy in the band and cross-hatched area drops from $\sigma 2\ N/2E$ to zero (this region is called the stress relief zone). Next, consider a geometrically similar panel. It is usually the case, that the larger the panel, the large the crack band and consequently the larger the cross-hatched area = in a larger structure, more energy is released in a strip by the same extension of the crack band. It is usually assumed that the edges of the specimen are fixed during the crack advance (displacement control), and so the external work is zero. The condition balancing the total energy released from the stress relief zone and the fracture energy needed to advance the crack by Δ*a* reads

$b(hf\Delta a + 2ka_0\Delta a)\sigma N\ 2\ /2E = Gfb\Delta a$.

Following Ba˘zant we further denote

$B_{f\,0} = \sqrt{G_f h_f}/E$ = const and

$D_0 = h_f D / 2\ ka_0$ = const

where f_0 is the tensile strength and D/a0 = const due to geometrical similarity. Combining the above expressions together with Eq. (85) gives the Ba˘zant size effect equation in the form

$$\sigma_{Nu} = Bf_0(1 + D/D0)$$

Note that both Bf 0 and D0 depend on the fracture properties of the material and on the geometry of the structure, but not on the structure size. Also not that equation is approximate, valid only within a range of about 1:20 for most structures.

The elastic stress and displacement field surrounding a non linear process zone correspond to a certain crack length a. In this case one can write

$a = a_0 + c$

where a_0 is the initial length on the notch or crack.

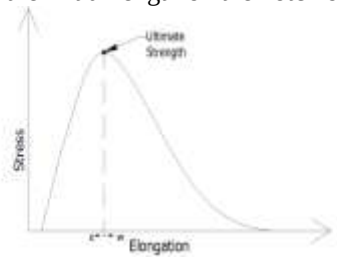

Fig. 1.5 Stress Elongation Curve

The fracture energy is a measure of the materials fracture toughness. It is important to note that, in addition to the fracture energy, this model requires that one must know the ultimate strength, and the shape of the fracture curve (Shah et al. 1995). Some state that since the fracture energy is a material property, it should be invariant with beam size (Muralidhara et al. 2011). However, because of the size effect the value of G_F may decrease with increasing size (Bazant and Planas 1998).

The length of the fracture process zone is termed the characteristic length and using this analysis can be estimated using the following relationship, where E is Young's modulus, G_f is the fracture energy, and f_t is the ultimate strength.

$$l_{ch} = (EG_f)/(f_t^2)$$

On an ending note, it has been pointed out that, in its formulation, Fictitious Crack Model can be applied to un-cracked as well as cracked structures (Gustafsson and Hillerborg 1985). This gives it an advantage over other fracture models that are only applicable for post crack behavior.

VIII. MODELING FRACTURE CURVE:

In the fictitious crack model, as mentioned, it is important to know the shape of fracture curve (stress-crack opening displacement curve) (Shah et al. 1995). Knowing the shape of the curve offers a description to the behavior of the energy dissipation process. Linear (Figure 1.7.2 a), bi-linear (Figure 1.7.2 b), exponential (Figure1.7.2 c), and power curves (Figure 1.7.2 d) are just a few of the common shapes used to describe the nature of this process (Shah et al. 1995). Each of these curves starts with the ultimate tensile stress ft at a crack opening of zero, and are terminated (zero stress) at some critical crack opening w_c.

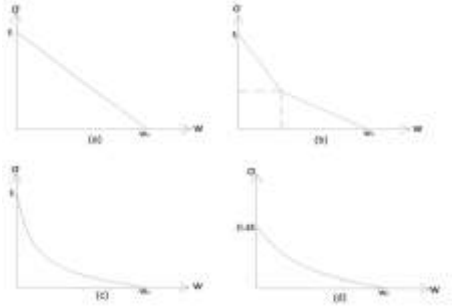

Fig: 1.6 Constitutive models

IX. FRACTURE BEHAVIOR

The quasi-brittle behavior of concrete can be best explained by the following five stages (Shah et al. 1995) as depicted graphically in figure 1.8 and with the use of figure1.8

Elastic:

The material exhibits elastic behaviour until the proportional elastic limit (PEL) is reached. The PEL in concrete is typically assumed to be the point of first crack (Shah et al. 1995).

Damage Localization:

The micro-cracks will localize forming a micro-crack, which occurs at the point of initial crack localization. At which point the material undergoes stable crack growth (crack propagates only when load increases) and a softening behavior occurs (Shah et al. 1995).

Unstable Crack Growth:

Once the ultimate strength is reached at a critical crack length the crack will undergo unstable growth (crack propagates even though load decreases) (Shah et al. 1995).

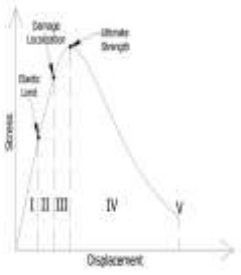

Fig.1.7 Stages of quasi-brittle behaviour

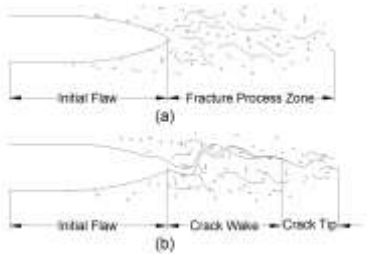

Fig. 1.7 Fracture process zone: stage II (a) and stage III (b)

For analysis purposes it is commonly assumed that a crack propagates in a linear fashion. However, concrete is a composite material so cracks tend to propagate along non-linear or chaotic crack paths due to the heterogeneity of the material. This can be associated with several toughening mechanisms that occur within the Fracture Process Zone (FPZ) as pointed out by Shah et al. (1995).

Micro crack Shielding:

Randomly oriented micro cracks occur at flaws ahead of the crack tip. The micro-cracking is caused by the high stress concentration near the crack tip (Shah et al. 1995). The formation of micro-cracks releases energy, which increases the amount of energy required to form unstable cracks (Anderson 2005).

Crack Deflection:

This occurs when inclusion (i.e., aggregates or fibers) is strong enough to divert the path of least resistance around the inclusion (Shah et al.1995).

X. FRACTURE MECHANICS OF CONCRETE

Concrete is a heterogeneous anisotropic non linear inelastic composite material, which is full of flaws that may initiate crack growth when the concrete is subjected to stress. Failure of concrete typically involves growth of large cracking zones and the formation of large cracks before the maximum load is reached. This fact and several properties of concrete, points toward the use of fracture mechanics. Furthermore, the tensile strength of concrete is neglected in most serviceability and limit state calculations. Neglecting the tensile strength of concrete makes it difficult to interpet the effect of cracking in concrete.

Two basic types of structural failure may be stated: brittle and plastic. Plastic failure occurs in materials with a long yield plateau and the structure develops plastic hinges. For materials with a lack of yield plateau, the fracture is brittle, which implies the existence of softening. During softening the failure zone propagates throughout the structure, so the failure is propagating.

In 1983 Wittmann suggested to differentiate between three different levels of cracking in concrete. The levels are categorized as follows:

1. Micro cracks that can only be observed by an electron microscope.
2. Meso cracks that can be observed using a conventional microscope.
3. Macro cracks that visible to the naked eye.

Micro cracks occur on the level of the hydrated cement, where cracks form in the cement paste. Meso cracks form in the bond between aggregates and the cement paste. Finally, macro cracks form in the mortar between the aggregates.

XI. THE FRACTURE PROCESS IN COMPRESSION

The compressive stress strain curve for concrete can be divided into four regions, see fig 1.3.1. The figure describes four different states of compressive cracking.

Initial cracks on the micro-level, caused by shrinkage, swelling, and bleeding, are observed in the cement paste prior to loading. For loads of approximately 0-30% of the ultimate load the stress strain curve is approximately linear and no growth of the initial cracks is observed. Between approximately 30-50% of the ultimate load a growth in bonding cracks between the cement paste and aggregates is observed. The curve is divided into four regions for different stages of cracking:

1. Pre existing bond cracks extend only slightly under load.
2. Slow growth of bond cracks.
3. Additional growth of bond cracks plus slow growth of matrix cracks.
4. Rapid growth of matrix cracks.

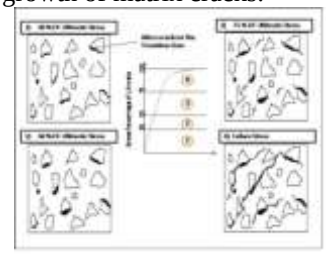

Fig: 1.8 The compressive stress- strain curve for concrete

XII. THE FRACTURE PROCESS IN TENSION

The tensile strength of concrete is much like the compressive strength, dependent on the strength of each link in the cracking process, i.e., micro cracks in the cement paste, meso cracks in the bond and macro cracks in the mortar. Consider a concrete rod under pure tensile loading. The fracture process initiates with crack growth of existing micro cracks at approximately 80% of the ultimate tensile load. This is followed by formation of new cracks and a halt in

formation of others due to stress redistribution and the presence of aggregates in the crack path. These cracks are uniformly distributed throughout the concrete beam. When the ultimate tensile load is reaches, a localized fracture zone will form in which a macro crack that splits the specimen in two will form. The fracture zone develops in the weakest part of the specimen.

XIII. TEST SETUP & TEST PROCEDURE

After 28days of curing the samples were taken out from the curing tank and kept for dry. Then notch is provided at one-third length of the beam with a/w i.e., notch depth to specimen depth ratio of 0.3, 0.4, 0.5, 0.6. After this the sample was coated with white wash. One day later the sample was kept for testing.

The notched beam specimen was kept on the supports of testing machine as shown in figure. Uniformly distributed load was applied over the central one third part between the notches and square cross section steel supports were provided at bottom along the outer edges of the notches as shown in figure, so that the central portion could get punched/sheared through along the notches on the application of loading. When performing a test, a gradually increased load is applied to the notched beam until a stress level is reached which results in crack propagation. With the increase of load propagation of these cracks in more or less vertical direction along with the formation of new cracks at the bottom of one or both the notches was observed. Finally the specimens failed by shearing along the notches.

Fig. 1.9 testing setup of notched beam specimen

The beam specimens were tested on the Universal Testing Machine of capacity 1000 Tons. All the beam specimens were tested under the four point bending test with the displacement rate control. A photograph of the Universal Testing Machine is shown in Fig 4.1. The Load and Displacement was measured by using the Universal Testing Machine.

XIV. SIZE EFFECT METHOD (SEM):

It may be noted that, the structural size effect is the most important manifestation of fracture phenomena. Geometrically similar specimens of concrete as a quasi-brittle material, exhibit a pronounced size effect on their failure loads. Therefore, it is worthwhile to relate the size effect behavior to the fracture properties of materials. SEM has been developed according to effective elastic crack model originally proposed by Bazant and Pfeiffer. This method has been included in RILEM TC-89. In this method, major fracture parameters are determined using three-point bending test on geometrically similar notched beams with varying sizes. Based on this method, nominal strength of geometrically similar concrete specimen can be described by size effect law as:

$\sigma_N = Bf_t/\sqrt{(1+B)}$;

Where $\beta = d/d_0$

In which σ_N = nominal stress at the maximum load Pu ($\sigma_N = c_nPu/bd.$); b = thickness of the specimen; d = size or characteristic dimension of the specimen (e.g., beam depth in bending test); c_n = coefficient introduced for convenience; B and d_0 are two parameters determined experimentally; and f_t is a measure of material strength, which can be taken as the tensile strength of the concrete. The theory is based upon three distinct types of fracture regimes, which are linear elastic fracture mechanics (LEFM), nonlinear fracture mechanics (NLFM) and strength theory, as illustrated in Fig. 14.

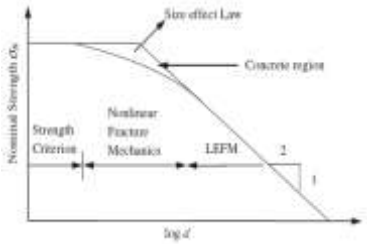

Fig. 1.10 The generalized size effect law

Therefore, Bazant and Kazemi concluded that if the peak loads of geometrically similar specimen with varying sizes are extrapolated to a specimen of infinite size, the obtained fracture energy is unique and is consequently independent of the specimen size and thus, LEFM assumptions can be used. Therefore, using linear regression of the peak loads of geometrically similar specimens of varying sizes, and according to size effect law Eq., the coefficients B and d_0 can be determined as:

$$Y = AX + C$$

In which: X = d, $Y = (f_t/\sigma_N)^2$, $B = 1/\sqrt{C}$ and d_0 = C/A the slope A and intercept C in the plot of Y vs. X can be used to determine the two parameters B and d_0 in the given equation. Based on the concept of LEFM, Bazant and Kazemi concluded that in failure

of structures of infinite size, the two major fracture parameters, fracture energy (G_f) and effective length of process zone (C_f) can be determined through:

$G_f = g(\alpha)/AE * f_t^2$ And $C_f = g(\alpha)/g'(\alpha_o) * C/A$

Where E is the modulus of elasticity of concrete, A is the angular coefficient of regression line; C is the y-intercept of the regression line, g(α) is the non-dimensional energy release rate and g'(α_0) is the derivative of g(α) with respect to the relative initial crack length ($\alpha_0 = a_0/d$). These functions (g(α) and g'(α)) are geometry dependent and obtained according to LEFM . g(α_0) , for some cases, can be found in RILEM-TC 89 recommendation. In SEM, other fracture parameters of interest including fracture toughness (K_{IC}) can be determined as:

$$K_{IIC} = \sqrt{EG_f}$$

XV. DETERMINATION OF FRACTURE PARAMETERS:

The Size Effect Law (SEL) which is applied to geometrically similar specimens of different sizes takes the form as shown below:

$$\sigma_N = Bf_t/\sqrt{(1+B)};$$

;Where $\beta = d/d_0$ (1)

The fracture energy (G_f) was obtained from the slope of the Regression line (A) and the elastic modulus (E) as given below:

$$G_f = g(\alpha)/AE * f_t^2$$

Where f_t = direct tensile strength, in absence of direct tensile test the value f_t is taken as 0.665 times the split tensile strength of concrete.

The effective length of Fracture Process Zone (C_f) was calculated by:

$$C_f = g(\alpha)/g'(\alpha_o) * C/A$$

Where

$$f(\alpha) = \frac{1.99-\alpha(1-\alpha)(2.15-3.93\alpha+}{(\sqrt{\pi})(1+2\alpha)(1-\alpha)^{3/2}}$$ for beams having geometry of S/D = 4. (5)

The stress intensity factor (K_I) was calculated by: $K_I = \sigma_N \times f(\alpha) \times \sqrt{\pi a_0}$

$$\sigma_N = \frac{Bf_t}{\sqrt{1+\beta}}$$

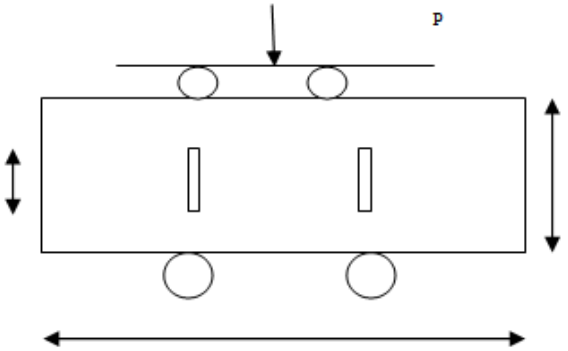

Fig 1.11: Specimen geometry for the four – point bending beams

XVI. TESTING PROGRAM and MATERIALS

The main ingredients used were cement, fine aggregate, coarse aggregate, water, and steel plates.

Cement

Ordinary Portland cement of 53 grade conforming to IS: 12269-1987 was used for the study.

Fine Aggregate

River sand passing through 4.75 mm sieve and conforming to grading zone II of IS: 383-1970 was used as the fine aggregate.

Coarse Aggregate

Crushed granite stone with a maximum size of 20 mm was used as the coarse aggregate.

Steel plates

Steel plates of 2 mm mean thickness and 22.5, 30, 37.5, 45, 60, 75, 90, 120, 150, 180mm in width were used at a/w ratios of 0.3, 0.4, 0.5, 0.6.

Water

Potable water supplied by the college was used in the work

Tamping Rod

Tamping rod was used for compacting the test specimens, beams.

Curing:

The specimens were removed from the moulds after 24 hours of casting and the specimens were placed in water for curing.

Preparing of Notch:

The notch was prepared with steel plates with different a/w ratio sizes.

XVII. MIX PROPORTIONING

The normal strength concrete mix M30 was proportioned as per Indian Standard for a target mean

strength 30MPa. After various trial mixes, the optimum mix proportion was selected as 0.45:1:1.562:2.902 with cement content of 405.81 kg/m^3. The different constituents in the order of water: cement: fine aggregate: coarse aggregate were proportioned as 183.0:406.81:635.4:1180.56 for making 1m^3 of mix. The steel plates were prepared with a/w ratios. The plates were placed at one-third of the length of the beam.

Fig 1.12universal testing machine

Fig.1.13 steel plate for notch

Fig. 1.14 wooden mould for large size beams

Fig.1.15 wooden mould for medium size beams

Fig .1.16 wooden mould for small size beams

XVIII. CALCULATIONS

The beam specimens were tested on the Universal Testing Machine under displacement rate control. All the beam specimens were tested under the three point bending under the displacement rate control. A photograph of the test setup is shown in Fig 4.0. To understand the fracture behavior of plain concrete beams the following graphs were drawn, Load Vs Mid span deflection (Fig 5.0, 5.1, 5.2). The normal and shear stress and stress intensity factor and fracture energy of the beams subjected to three point bending with eccentric notch calculated by using the

eq.s (5.1 to 5.8) from reference (1) and reported in Table 5.0 and in table 5.1. From the graphs and Tables it was observed that, for mixed-mode failure of concrete, It was found that the stress intensity factor and fracture energy increases with the increasing of beam sizes and decreasing the failure stresses with increasing the beam sizes. The brittleness of the beam increases with increase the size of the beam.

For the calculation of the stress intensity factor the following formulae can be used for mode – II

$$G_{II} = \frac{(1-\mu^2)\,K^2_{II}}{E}$$

$$K^2_{II} = \frac{G_{II} * E}{(1-\mu^2)}$$

Where

$$GII = \frac{W_{FS}}{A_{eff}}$$

W_{FS} = work of fracture in mode II, calculates as the area under the load – slip curve.

A_{eff} = effective area of cross section of the specimen.

μ = poisons ratio for concrete = 0.3

E = young's modulus of the concrete

S. No	Size of the beam	a/w ratio	Ultimate load(KN)	Shearstress (τ_N)n/mm^2
1	1000*300*75	0.3	209.55	13.3
		0.4	184.20	13.6
		0.5	180.10	16.0
		0.6	165.80	18.42
2	500*150*75	0.3	55.60	7.06
		0.4	53.50	7.97
		0.5	52.30	9.29
		0.6	42.30	9.4
3	250*75*75	0.3	40.80	10.36
		0.4	37.50	11.11
		0.5	35.80	12.70
		0.6	32.70	14.53

Table 1.1 Failure stresses

Graphs for Load vs Displacement FOR SMALL SIZE BEAMS

GRAPH FOR 0.3(NOTCH SIZE: 22.5MM)

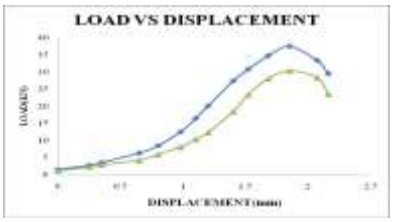

S. No	Size of the beam	a/w ratio	Fracturee nergy (G)N/mm	Stress intensity factor(K) N/mm $^{1.5}$
1	1000*300*75	0.3	27.32	901.31
		0.4	28.33	917.85
		0.5	25.75	866.78
		0.6	24.21	849.03
2	500*150*75	0.3	6.87	424.51
		0.4	12.76	600.81
		0.5	8.67	490.94
		0.6	7.23	465.43
3	250*75*75	0.3	14.72	649.02
		0.4	12.60	600.87
		0.5	12.60	615.71
		0.6	10.47	559.32

Table 1.2: Fracture Energy and Stress intensity factors

GRAPHS FOR 0.4(NOTCH SIZE: 30MM

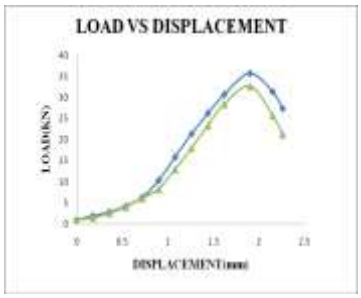

GRAPHS FOR 0.5(NOTCH SIZE: 37.5MM)

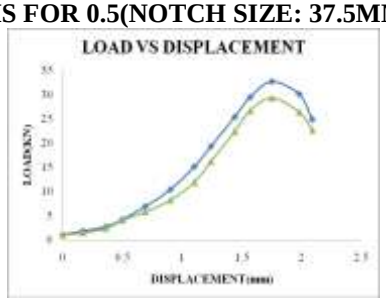

GRAPHS FOR 0.6(NOTCH SIZE: 45MM) FOR MEDIUM SIZE BEAMS

GRAPHS FOR 0.3(NOTCH SIZE: 45MM)

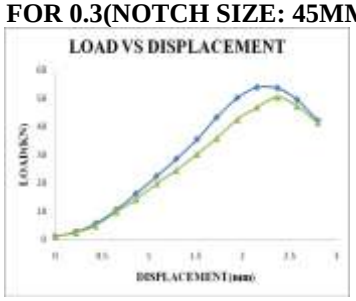

GRAPHS FOR 0.4(NOTCH SIZE: 60MM)

GRAPHS FOR 0.5(NOTCH SIZE: 75MM)

GRAPHS FOR 0.6(NOTCH SIZE: 90MM) FOR LARGE SIZE BEAMS

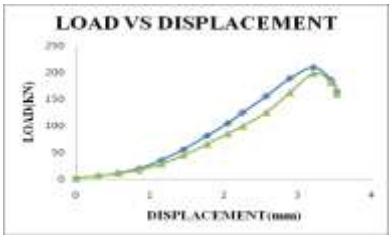

GRAPHS FOR 0.3(NOTCH SIZE: 90MM)

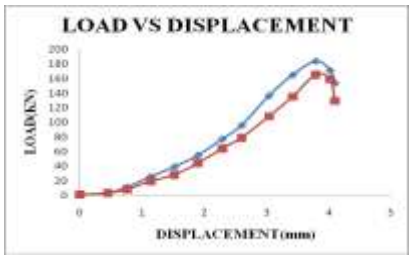

GRAPHS FOR 0.4(NOTCH SIZE: 120MM)

GRAPHS FOR 0.5(NOTCH SIZE: 150MM)

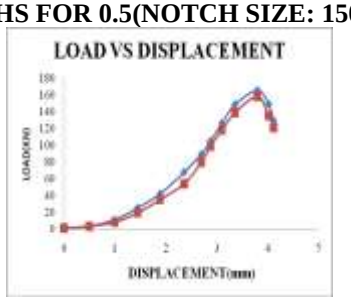

GRAPHS FOR 0.6(NOTCH SIZE: 180MM)
Fig:1.17 Graphs for load vs displacement for all sizes of beams

Load Vs shear stresses for all a/w ratio of all sizes of beam

Graph for 0.3 a/w ratio for all sizes of beams

Graph for 0.4 a/w ratio for all sizes of beams

Graph for 0.5 a/w ratio for all sizes of beams

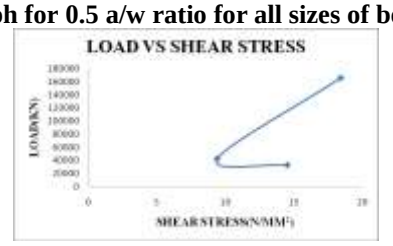

Graph for 0.6 a/w ratio for all sizes of beams
Fig 1.18 Graphs for load vs shear stress of a/w ratio of all sizes of beams

Graphs for Fracture energy vs a/w ratio of all sizes of beams

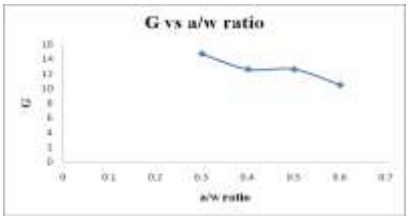

Graph for G vs a/w ratio of small size beams

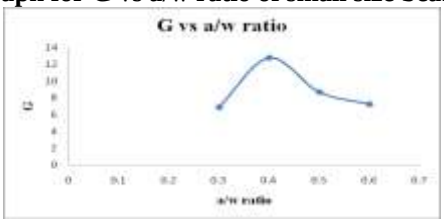

Graph for G vs a/w ratio of medium size beams

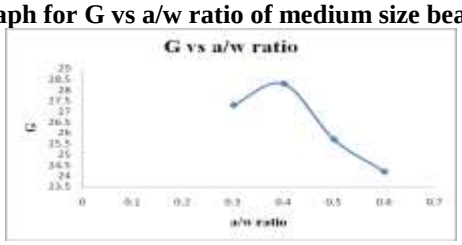

Graph for G vs a/w ratio for large size beams
Fig 1.19 Graphs for G vs a/w ratio for all sizes of beams

Graph for stress intensity factor vs a/w ratio of all sizes of beams

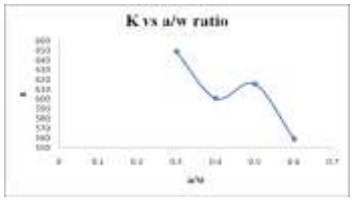

Graph for K vs a/w ratio for small size beams

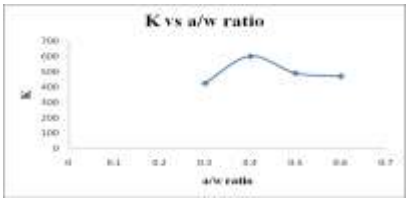

Graph for K vs a/w ratio for medium size beams

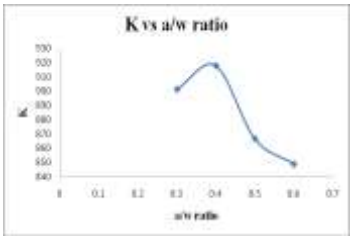

Graph for K vs a/w ratio for large size beams

XIX. CONCLUSIONS

Based on the tests on twenty four double centered notched concrete beam specimens, the following conclusions have been drawn

1. From tests we observe that the failure stresses increases with increase in beam sizes.
2. Fracture toughness or stress intensity factor increases up to certain point and then decreases with increase in notch depth for all sizes of beams.
3. Fracture energy or energy release rate increases up to certain point and then decreases with increase in notch depth for all sizes of beams.
4. For constant notch to depth ratio of beam size increases with decrease in stress intensity factor.
5. For constant notch to depth ratio of beam size increases with decrease in fracture energy.
6. It is observed that the load increases with decrease in notch size.
7. It is observed that the load decreases with increase in failure stresses.
8. For constant notch to depth ratio of beam sizes the failure stresses decreases.

REFERENCES

[1.] Agarwal, B.D. and Giare, G.S., "Fracture toughness of short-fiber composites in Modes-I and II", Engineering Fracture Mechanics, Vol. 15, No. 1, 1981, pp.219-230.

[2.] Bazant , Z.,p, and Pfeiffer, P.A., "Shear fracture tests of concrete", materials and structures (RKLEM) , 1984, vol. 19, pp.111-121.

[3.] Watkins, J. and Liu, K.L.W., "A Finite Element Study of Short Beam Test Specimens under Mode-II loading", The International Journal of Cement Composites and Light Weight Concrete, Vol.7, No.1, Feb.1985, pp.39-47.

[4.] Bazant , Z.,p, and Pfeiffer, P.A., "Tests on shear fracture and strain softening in concrete", proceedings of second symposium on interaction of Non-nuclear Munition with structures Florida, USA, April 1985, pp. 254-264.

[5.] Davies, J., Yim, C.W.A and Morgan, T.G., "Determination of Fracture parameters of punch through shear specimens", The International Journal of Cement Composites and Light weight Concrete, Vol. 9, No. 1, Feb. 1987, pp. 33-41.

[6.] BhaskarDesai . V, "Some studies on Mode - II fracture and stress – strain behavior in shear of cementitious materials", Ph.D thesis, Indian Institute of Science, Banglore".

[7.] PrakashDesayi, Raghu Prasad .B.K, and Bhaskar Desai . V, "Experimental determination of KIIc from compliance and fracture energy", proceedings national seminar on Aerostructures, organized by IIT, Kanpur, India, 29-30, Dec, 1993, pp. 33-34.

[8.] Prakashdesayi, B.K.Raghu Prasad and V.Bhaskar Desai, "Mode – II fracture of cementitious materials- part – I : Studies on specimens of some new geometries", Journal of Structural Engineering, Vol.26, No.1, April 1999, pp.11-18.

[9.] Prakashdesayi, B.K.Raghu Prasad and V.Bhaskar Desai, "Mode – II fracture of cementitious materials- part – II: Fracture toughness of cement paste, mortar, concrete and no-fines concrete. Journal of structural engg Vol. 26, No. 1, April 1999, pp. 19-27.

[10.] Prakashdesayi, B.K.Raghu Prasad and V.Bhaskar Desai, "Mode – II fracture of cementtiotus materials- part – III: Studies on shear strength and slip of cement paste, mortar, concrete and no-fines concrete. Journal of structural engg Vol. 26, No.2, July 1999, pp. 91-97.

[11.] Prakashdesayi, B.K.Raghu Prasad and V.Bhaskar Desai, conducted Mode-II fracture of cementitious materials- part-IV: Fracture toughness, shear strength and slip of fibre reinforced cement mortar and concrete. Journal of structural engg. Vol. 26, No. 4, Jan 2000, pp. 267-273.